Kinetics of Oxygen-Induced Faceting of Vicinal Ag(110)

J. S. Ozcomert,[1,2] W. W. Pai,[1] N. C. Bartelt,[1] and J. E. Reutt-Robey[2]
[1]*Department of Physics, University of Maryland, College Park, Maryland 20742*
[2]*Department of Chemistry, University of Maryland, College Park, Maryland 20742*
(Received 26 August 1993)

The oxygen-induced breakup of vicinal Ag(110) surfaces into (110) facets and step bunches is measured with scanning tunneling microscopy. Faceting transitions are recorded in real time at room temperature for two surface orientations. A vicinal Ag(110) surface misoriented by 2° towards [001] facets via the growth of isolated nuclei. Step-position fluctuations of increasing magnitude are observed prior to faceting, revealing a critical terrace width of ~100 Å. In contrast, oxygen exposure causes Ag(110) misoriented by 2° towards [3$\bar{3}$1] to facet spontaneously with no evident nucleation barrier.

PACS numbers: 68.35.Md, 61.16.Ch, 81.60.Bn, 82.65.Dp

Many surfaces exhibit dramatic morphological changes upon chemical adsorption [1–5]. In extreme cases single-crystal surfaces of arbitrary orientation can even facet, or break up, into regions of two or more different orientations. Understanding the orientational stability of single-crystal surfaces with respect to chemical adsorption has been a fundamental issue in surface physics for more than forty years [1,3,6,7]. Previous studies of faceting [5,8] have focused primarily on the equilibrium thermodynamics of the transformation. The thermodynamic criteria for faceting to occur are well established [6]. As discussed in more detail below, adsorption induces faceting by changing the dependence of the free energy on surface orientation. Much less is known about the kinetics of these gross morphological rearrangements, however. Unfortunately, a *post facto* structural analysis of a faceted surface cannot determine the faceting mechanisms unambiguously. The advent of rapid microscopic techniques to monitor surface structure now permits dynamic observations of faceting [9–11]. In the present paper, we report the first microscopic measurements of adsorbate-induced faceting. Structural details of the room-temperature faceting of two vicinal Ag(110) surfaces upon oxygen adsorption are determined directly from scanning tunneling microscopy (STM) measurements of the same surface region taken as a function of time.

The O/vicinal-Ag(110) system was selected for these studies to permit measurements of faceting kinetics at room temperature. Previous STM [12,13] investigations involving silver surfaces have shown substantial mobility of surface silver atoms even at 300 K. In addition, low-energy electron diffraction (LEED) investigations of Ag(331) have revealed room temperature faceting to the (110) orientation on a time scale of hours following exposure to oxygen [14]. On the (110) surface, oxygen forms a series of $(n\times 1)$ reconstructions [15].

Studies are performed on single-crystal silver surfaces slightly misoriented from the (110) direction. The STM measurements are conducted in an ultrahigh vacuum system on samples which are initially cleaned by many cycles of argon ion sputtering, annealing, mild oxidation, and annealing at 600 K. After the sample is permitted to equilibrate to 300 K, and continuous series of >100 large area images is collected while a constant background oxygen pressure is introduced.

Representative STM topographs obtained upon exposing the Ag(110)2° → [001] surface to a 1×10^{-8} torr O_2 pressure are shown in Fig. 1. Prior to exposure, the surface consists of an array of monatomic steps separated by

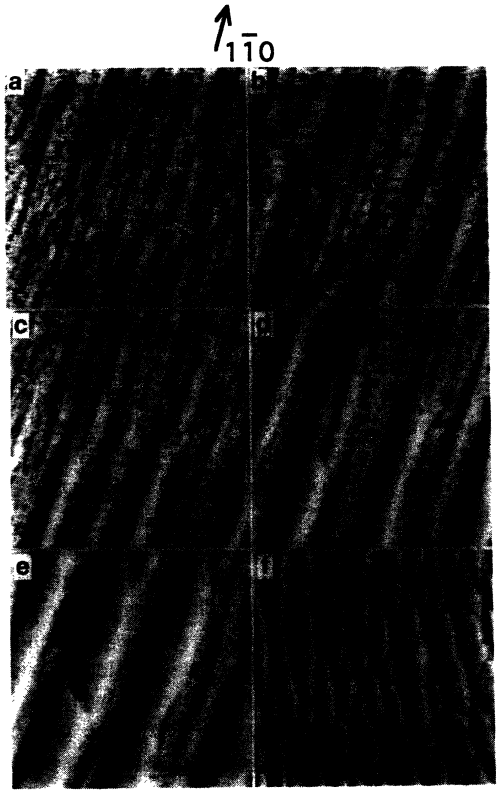

FIG. 1. STM sequence for faceting of Ag(110)2° → [001], showing the nucleation and growth of isolated facets during exposure to 1×10^{-8} torr of O_2 with a 1500 Å×1500 Å field of view: (a) the clean surface with steps along [1$\bar{1}$0]; (b) after 85 min (50 L); (c) after 125 min (73 L); (d) after 160 min (94 L); (e) after 260 min (152 L); (f) final large scale, 4000 Å×4000 Å image.

0031-9007/94/72(2)/258(4)$06.00

(110) terraces of 35 Å average width [Fig. 1(a)]. The distribution of terrace widths on the clean surface, with terrace widths fluctuating between 0 and 80 Å, is characteristic of steps which interact primarily via entropic repulsions [16]. The step edge frizziness in these relatively slow scans can be attributed to rapid kink motion [17] or adatom attachments/detachments. After oxygen exposure is initiated, the distribution of terrace widths becomes increasingly broad [Fig. 1(b)], although no facets are observed for the first 85 min [50 langmuir (L, 1 L $=10^{-6}$ torrs) O_2 exposure]. The largest terrace observed during this period is ca. 80 Å wide. Continuous fluctuations cause these large terraces to shrink as others grow. As exposure to oxygen further increases to 54 L, the fluctuations increase in amplitude, generating terraces approximately 100 Å wide. It is these large terraces that nucleate the formation of linear (110) facets, as shown in Fig. 1(c). Smaller scale images reveal the presence of a (7×1) reconstruction on these nucleated (110) facets. With increasing time (and oxygen exposure) the facets grow and become more distinct, appearing as long stripes diagonally crossing the frames [Fig. 1(d)]. The long facet edges lie predominantly parallel to the close-packed [1$\bar{1}$0] direction. At yet longer times, the individual facets collide and approach their final size [Fig. 1(e)]. The final surface consists of long 300 Å wide facets separated by step bunches comprised of approximately close-packed steps. The (110) facets are covered by a (3×1) oxygen overlayer, as determined by LEED and STM. The basic mechanism for this process—the initial appearance of random isolated facets which grow in size as new facets appear—is characteristic of a phase separation which proceeds by nucleation. Similar results are observed on this surface for oxygen pressures ranging from 5×10^{-9} to 5×10^{-8} torr.

We now discuss how the fluctuations in step position *prior* to faceting reveal how the free energy of the surface is changing with respect to oxygen adsorption. The projected free energy per area of a vicinal surface, f, can be expressed in terms of the step density or tangent of the miscut angle ρ as

$$f=f^0+\beta\rho/h+g\rho^3/h^3, \quad (1)$$

where f^0 is the free energy of the low index surface, β is the step formation energy per unit length, g represents the step-step interaction energy, and h is the step height. A requirement for a thermodynamically stable surface is that the free energy be everywhere a convex upwards function of ρ [18], that is the surface stiffness κ_x must be positive:

$$\kappa_x=\frac{\partial^2 f}{\partial\rho^2}=\frac{6g\rho}{h^3}>0. \quad (2)$$

A schematic evolution of the variation of $f(\rho)$ with oxygen adsorption which violates this condition and thus leads to faceting is shown in Fig. 2. Prior to oxygen adsorption, the free energy of the vicinal surface increases monotonically with miscut angle, as expected from Eq. (1) for steps which interact through their entropic repulsions. As oxygen is adsorbed, the free energy decreases. However, because different orientations will be covered by different amounts of oxygen [19] the amount of change depends upon miscut angle, changing the orientational dependence of the surface free energy. Large amounts of O adsorption on the (110) surface eventually cause the convexity condition of Eq. (2) to fail, after which the surface to break up into orientations specified by the end points of the dashed tie lines of Fig. 2.

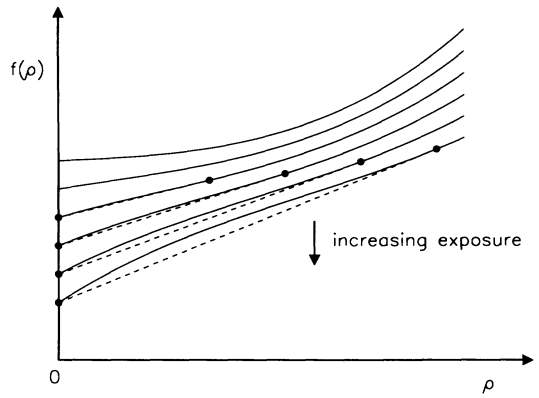

FIG. 2. Schematic illustration of the change in free energy f upon oxygen adsorption as a function of step density ρ. The uppermost curve, which is concave up and thus thermodynamically stable, portrays the clean surface. Increasing exposure to oxygen causes the number of oxygen atoms on the surface to increase, increasing the surface chemical potential [19]. Preferential adsorption on (110) planes eventually leads to a free energy curve which is not convex, and thus is unstable. Faceting produces the orientations specified by the end points of the dashed tie lines.

Inspection of Fig. 2 shows that before the surface becomes unstable with respect to faceting, the curvature of f with respect to ρ, i.e., κ_x, will decrease. Since κ_x determines the "compressibility" of the steps, a reduction in κ_x implies a reduction in the cost in free energy for pushing steps together or spreading them apart. Thus, thermal fluctuations in f on the oxygen-covered surface should generate larger terrace widths than those accessible on the clean surface. Consequently, larger fluctuations in step edge positions are expected before faceting occurs. This thermodynamic model can be tested by monitoring the fluctuations in a step edge position as the surface becomes covered with oxygen.

To quantify the step fluctuations, the step position correlation function $G(n)$ is computed directly from the STM images. This function is defined as $G(n)=\langle(x(n)-x(0)-ln)^2\rangle$, where the x direction is perpendicular to the step edges, n indexes the step edges, and l is the average terrace length. Figure 3 shows the average values for $G(n)$ calculated from ~200 measured step positions at four different times. The lower three curves are for times corresponding to 0, 25, and 45 L net O_2 exposure, before any facets have nucleated. A consistent increase in $G(n)$

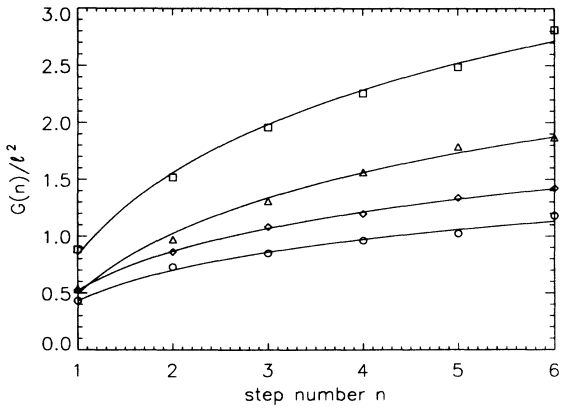

FIG. 3. Time evolution of the fluctuations in step edge position of the surface in Fig. 1, as measured by the step correlation function $G(n)$. The solid lines show fits by Eq. (3). [Circles: clean surface; diamonds: after 42 min (25 L); triangles: after 75 min (45 L); squares: after 100 min (60 L).]

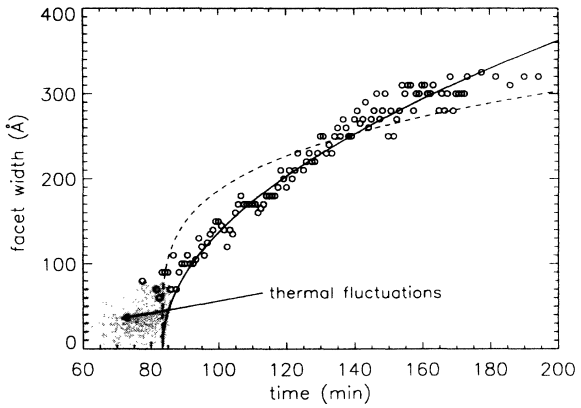

FIG. 4. The width of the central facet in Fig. 1 (circles) as a function of time after O_2 exposure. The facet growth rate is roughly consistent with a $t^{1/2}$ law (solid line), but not to a $t^{1/4}$ law (dashed line). The shaded 0–80 Å region denotes the terrace widths sampled through fluctuations prior to faceting.

is observed, corresponding to increasing step edge fluctuations. The uppermost curve is obtained just after faceting has started, as in Fig. 1(c). Clearly the surface does become rougher, as expected by the thermodynamic model.

This observation can be made more quantitative. The capillary wave theory of vicinal surfaces predicts that $G(n)$ should diverge logarithmically with distance n, with an amplitude which depends on the surface stiffness [20]:

$$G(n) \approx (2kTl^2/\pi\sqrt{\kappa_x\kappa_y})\ln(n) + C, \quad (3)$$

where κ_y is the surface stiffness along the step edges (which is proportional to the step edge stiffness, and thus determined by the kink energy). The solid lines in Fig. 3 show fits to this form with C and $\kappa_x\kappa_y$ as adjustable parameters. In the sequence of exposures shown in Fig. 3, the fitted value of $\kappa_x\kappa_y/(kT)^2$ decreases from the clean surface value of 2.6, to 1.6 after 42 min (25 L), to 0.7 after 75 min (45 L), just before the transition. Thus, the surface stiffness has decreased from its clean surface value by about a factor of 4 just before the surface facets.

To justify this treatment of faceting in terms of the thermodynamic and statistical mechanical theories of surface behavior, it is essential to establish that the surface can obtain thermal equilibrium. Two strong pieces of evidence indicate that these surfaces are in equilibrium. First, the terraces fluctuate on the order of their width on a time scale (seconds) much shorter than our observation time scale (hours). Second, we are able to reverse the faceting by removing the oxygen by exposing the surface to CO at *room temperature* [21]. This reversibility (and hence path independence) is the signature of an equilibrium process. It rules out, for example, the possibility that the oxygen simply enables faceting by increasing surface mobilities.

In principle, the fundamental mechanisms for mass flow during faceting can also be deduced from these STM measurements. For example, the theory of surface diffusion limited growth of isolated facets [22] predicts that the facet width should grow as $t^{1/4}$, whereas growth which is limited by the rate of attachment and detachment from step edges should follow a $t^{1/2}$ growth law [22]. As shown in Fig. 4, oxygen-induced facets on Ag(110)2° → [001] is more consistent with a $t^{1/2}$ size dependence, suggesting that the movement of step edges is limited by attachment processes along the step edge.

Finally, we show that this phase separation depends sensitively on the orientation of the step edge. In the faceting sequence described above, the vicinal Ag(110) surface facets by the nucleation of (110) facets when the terrace width becomes greater than 100 Å. We propose that this critical terrace width is determined by how the oxygen chains composing the $(n\times1)$ reconstructions form on the (110) terraces. For Ag(110)2° → [001] these chains are perpendicular to the step edges, suggesting that the critical terrace width is related to the shortest stable oxygen chain. One might then expect a change in the process of facet formation if the chains were not perpendicular to the steps. As we now show, a vicinal Ag(110)2° → [3$\bar{3}$1] surface composed of lower symmetry steps does facet in a distinctly different way upon oxygen adsorption. The step edges on this surface are rotated 7° from the [001] direction (i.e., next-nearest-neighbor [001] steps with a kink located every sixth atom along the step edge).

A faceting sequence of Ag(110)2° → [3$\bar{3}$1] subject to a 3×10^{-8} torr O_2 environment is shown in Fig. 5. The clean surface [Figs. 5(a) and 5(b)] appears very similar to the Ag(110)2° → [001] surface of Fig. 1(a). However, coincident with the start of oxygen exposure, a number of uniformly growing terraces appear simultaneously on the surface. The surface after 50 L exposure is shown in Fig. 5(c). The different facets grow in size virtually at the same rate with a regular periodicity that is evident almost immediately [Fig. 5(d)] (and conformed by Fourier analysis). At longer times, the structure of the facets becomes much sharper [Fig. 5(e)], yet the periodicity is not

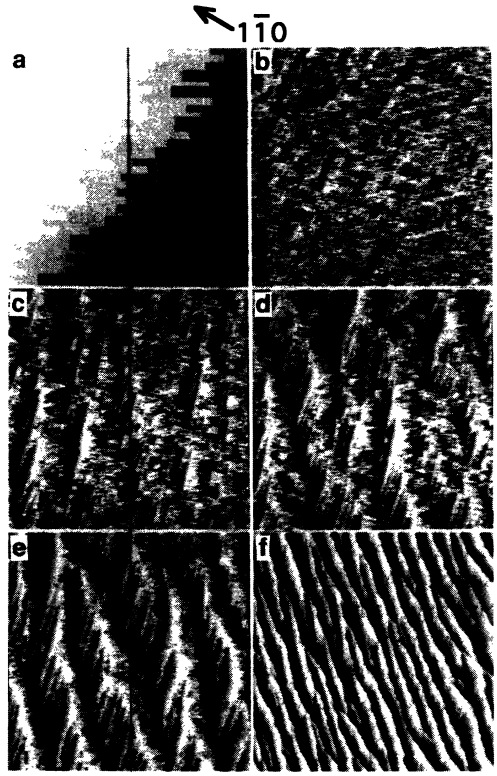

FIG. 5. STM sequence for Ag(110)2° → [3$\bar{3}$1] showing the instability of the surface with respect to the formation of facets under exposure to 3×10^{-8} O_2: (a) 150 Å×150 Å image of the clean surface (contrast is enhanced to delineate terraces); (b) the clean surface [frames (b)–(e) have a 1500 Å×1500 Å field of view]; (c) after 59 min (53 L); (d) after 70 min (71 L); (e) after 100 min (125 L); (f) final large scale, 5000 Å×5000 Å image [this frame is rotated by 20° from (a)–(e)].

changed. The emergent 200 Å wide (110) facets are separated by bunches of approximately ten steps. The main structural difference is that the (110) facets are crossed by a number of monatomic steps with step edges along [001]. Thus, the kinks initially in the step edges have been expelled from these steps, "precipitating" [23] into the step bunches. As anticipated from the discussion in the preceding paragraph, we attribute this expulsion to the desire of the O atoms to form long chains along [001] [12]: Kink expulsion increases the longest possible O chain length. The absence of a critical terrace width results from the fact that long O chains can form on these terraces before colliding with the step edges. The mechanism for the faceting of Ag(110)2° → [3$\bar{3}$1]—the spontaneous decomposition into a surface with a characteristic periodicity—indicates a surface which is kinetically unstable with respect to oxygen adsorption; i.e., the surface is undergoing spinodal decomposition [24].

In summary, we have measured the oxygen-induced faceting kinetics of two vicinal Ag(110) surfaces. Faceting occurs at oxygen coverages less than that of the (7×1) reconstruction. The nature of the faceting transition is sensitive to surface orientation. A vicinal Ag(110) surface comprised of 35 Å wide terraces separated by close-packed steps facets slowly by nucleation. The time evolution of the fluctuations in step edge positions reveals that fluctuations in terrace width are amplified by the adsorption of oxygen. In contrast, a vicinal Ag(110) surface comprised of 35 Å wide terraces separated by low symmetry steps facets spontaneously upon oxygen adsorption.

This work was supported by NSF-MRG Grant No. DMR91-03031 and a Packard Foundation Fellowship. We are indebted to Ellen Williams and Ted Einstein for many useful discussions.

[1] A. J. W. Moore, in *Metal Surfaces*, edited by W. D. Robertson and N. A. Gjostein (American Society for Metals, Metals Park, OH, 1962), p. 155.
[2] G. A. Somorjai and M. A. Van Hove, Prog. Surf. Sci. **30**, 201 (1989).
[3] M. Flytzani-Stephanopoulos and L. D. Schmidt, Prog. Surf. Sci. **9**, 83 (1979).
[4] E. D. Williams and N. C. Bartelt, Ultramicroscopy **31**, 36 (1989).
[5] T. E. Madey, K.-J. Song, and C.-Z. Dong, Surf. Sci. **247**, 175 (1991).
[6] C. Herring, Phys. Rev. **82**, 87 (1951).
[7] E. D. Williams and N. C. Bartelt, Science **251**, 393 (1991).
[8] R. J. Phaneuf, E. D. Williams, and N. C. Bartelt, Phys. Rev. B **38**, 1984 (1988).
[9] R. J. Phaneuf *et al.*, Phys. Rev. Lett. **21**, 2986 (1991).
[10] M. Suzuki *et al.*, J. Vacuum Sci. Technol. **11**, 1640 (1993).
[11] H. Hibino *et al.*, Phys. Rev. B **47**, 13027 (1993).
[12] M. Taniguchi *et al.*, Surf. Sci. **262**, L123 (1992).
[13] M. Poensgen *et al.*, Surf. Sci. **274**, 430 (1992).
[14] R. A. Marbrow and R. M. Lambert, Surf. Sci. **71**, 107 (1978).
[15] H. A. Engelhardt and D. Menzel, Surf. Sci. **57**, 591 (1976).
[16] J. S. Ozcomert *et al.*, Surf. Sci. **293**, 183 (1993).
[17] M. Giesen *et al.*, J. Vacuum Sci. Technol. A **10**, 2597 (1992).
[18] A. A. Chernov, Usp. Fiz. Nauk **73**, 277 (1961) [Sov. Phys. Usp. **4**, 116 (1961)].
[19] We suppose that the oxygen mobility is large so that equilibrium is maintained across the surface. Hence there is a well defined chemical potential along the surface. Each curve in Fig. 2 corresponds to a different oxygen chemical potential.
[20] J. Villain, D. R. Grempel, and J. Lapujoulade, J. Phys. F **15**, 809 (1985).
[21] J. S. Ozcomert, W. W. Pai, N. C. Bartelt, and J. E. Reutt-Robey (to be published).
[22] W. W. Mullins, Philos. Mag. **6**, 1313 (1961).
[23] J. Wei *et al.*, J. Chem. Phys. **94**, 8384 (1991).
[24] J. Stewart and N. Goldenfeld, Phys. Rev. A **46**, 6505 (1992).

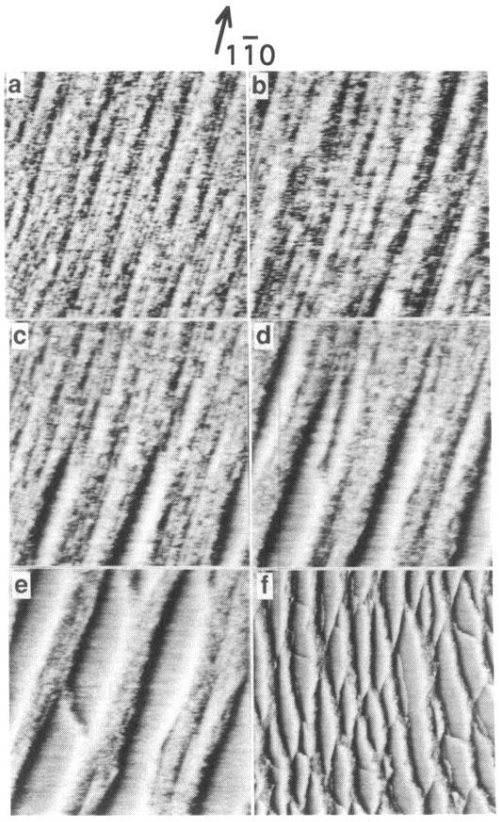

FIG. 1. STM sequence for faceting of Ag(110)2° → [001], showing the nucleation and growth of isolated facets during exposure to 1×10^{-8} torr of O_2 with a 1500 Å×1500 Å field of view: (a) the clean surface with steps along [1$\bar{1}$0]; (b) after 85 min (50 L); (c) after 125 min (73 L); (d) after 160 min (94 L); (e) after 260 min (152 L); (f) final large scale, 4000 Å×4000 Å image.

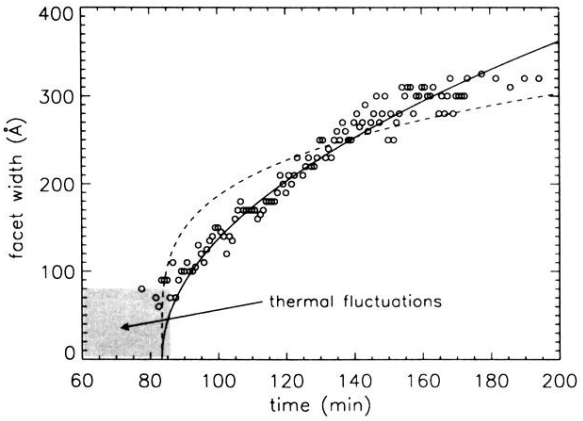

FIG. 4. The width of the central facet in Fig. 1 (circles) as a function of time after O_2 exposure. The facet growth rate is roughly consistent with a $t^{1/2}$ law (solid line), but not to a $t^{1/4}$ law (dashed line). The shaded 0–80 Å region denotes the terrace widths sampled through fluctuations prior to faceting.

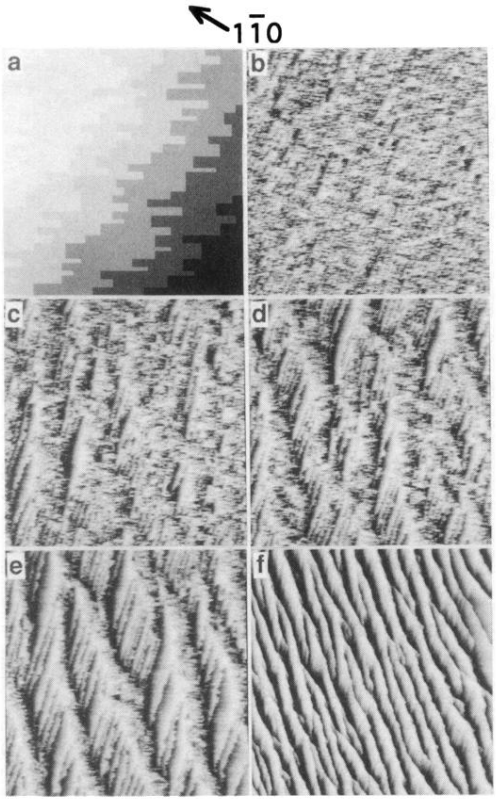

FIG. 5. STM sequence for Ag(110)2° → [3$\bar{3}$1] showing the instability of the surface with respect to the formation of facets under exposure to 3×10^{-8} O_2: (a) 150 Å×150 Å image of the clean surface (contrast is enhanced to delineate terraces); (b) the clean surface [frames (b)–(e) have a 1500 Å×1500 Å field of view]; (c) after 59 min (53 L); (d) after 70 min (71 L); (e) after 100 min (125 L); (f) final large scale, 5000 Å×5000 Å image [this frame is rotated by 20° from (a)–(e)].